Tighter Binding of HIV Reverse Transcriptase to RNA−DNA versus DNA−DNA Results Mostly from Interactions in the Polymerase Domain and Requires Just a Small Stretch of RNA−DNA†

William P. Bohlayer and Jeffrey J. DeStefano*

Department of Cell Biology and Molecular Genetics, University of Maryland, College Park, Maryland 20742

Received September 1, 2005; Revised Manuscript Received February 3, 2006

ABSTRACT: Binding of HIV reverse transcriptase (RT) to unique substrates that positioned RNA−DNA or DNA−DNA near the polymerase or RNase H domains was measured. The substrates consisted of a 50 nucleotide template and DNA primers ranging from 23 to 43 nucleotides. Five different types of template strands were used: homogeneous (1) RNA or (2) DNA, (3) the first 20 5′ nucleotides of DNA and the last 30 RNA, (4) the first 20 RNA and the last 30 DNA, and (5) 15 nucleotides of DNA followed by 5 RNA and then 30 DNA. The different length primers were designed to position RT over various regions of the template. Dissociation rate constants were determined for each of the substrates. Results showed that the severalfold tighter binding to RNA−DNA vs DNA−DNA was determined by binding in the polymerase domain and required only a short 5 base pair RNA−DNA hybrid region. Chimeric substrates with RNA−DNA positioned near the polymerase domain and DNA−DNA near the RNase H domain showed binding comparable to a complete RNA−DNA substrate, while those with the reverse orientation were comparable to DNA−DNA. Interestingly, the first configuration, though binding as tightly as RNA−DNA, could not be cleaved by RT RNase H activity, a finding that could perhaps be exploited in the development of nucleic acid-based inhibitors.

The retrovirus reverse transcriptase (RT)[1] is a multifunctional enzyme that possesses both RNA- and DNA-dependent DNA polymerase activity and an RNase H activity which degrades RNA that is part of an RNA−DNA hybrid (*1*−*3*). The two activities reside in different subdomains of the protein, and the catalytic sites are separated by approximately 18 nucleotides with the RNase H active site 18 bases behind the 3′ primer terminus when RT binds primer-templates (*4*−*10*).

Several studies have addressed RT's binding stability and orientation on different nucleic acid structures. General conclusions are as follows: (1) RT binds RNA−DNA hybrids much more tightly than DNA−DNA or RNA−RNA (*11*−*13*). (2) RT's pol domain binds to the 3′ end of short DNAs recessed on longer RNA or DNA templates in a classical primer-extension configuration, while short RNAs recessed on longer DNAs are bound at the 5′ end and recognized as substrates for RNase H cleavage rather than primers for extension (*14*−*16*). An exception to this is the polypurine tract (ppt) which is bound at the 3′ end and recognized as a primer (for a review see ref *17*). (3) Mutagenic analysis and crystal structures of HIV-RT bound to primer-templates have shown that numerous contacts occur throughout the enzyme including contacts in the polymerase and RNase H domains, but there are more contacts in the pol domain which presumably contributes more to substrate binding (*9*, *10*, *17*−*26*).

The ability of RT to bind RNA−DNA tighter than DNA−DNA is due at least in part to the different hybrid structures and the numerous additional contacts RT makes with RNA nucleotides, especially 2′-hydroxyl groups (*19*, *22*) (see Discussion). Still it is not known if the polymerase and RNase H domains of RT contribute differentially. For example, since the RNase H domain uses RNA−DNA exclusively while the pol domain can use DNA−DNA, RNA−DNA, or RNA−RNA as a substrate, tighter binding of RNA−DNA to the RNase H domain might be expected. Also, as noted above several additional interactions occur with RNA−DNA hybrids and many of these lie outside the pol domain (*22*; see Discussion). The relative contribution of the RNase H domain to the tight binding of RNA−DNA is unclear; however, results suggest that this domain also contributes to binding and positioning. Some RNase H mutants including D443N, D498N, and H539D also modestly affect polymerase activity (*27*, *28*). Some mutations in amino acids in the "RNase H primer grip" region, which is in the connection domain between the pol and RNase H active sites, affect both polymerization and RNase H (*29*−*31*). The RNase H active site mutant D443N and the E478Q mutant used here actually bind more tightly to the primer-template than wild type with low concentrations or in the absence of Mg^{2+}, while binding is equivalent when optimal Mg^{2+} (4−6

† This work was supported by National Institute of General Medicine Grant GM051140.

* Corresponding author: phone, 301-405-5449; fax, 301-314-9489; e-mail, jdestefa@umd.edu.

[1] Abbreviations: HIV, human immunodeficiency virus; RNase H, ribonuclease H; pol, polymerase; RT, reverse transcriptase; nt(s), nucleotide(s); ppt, polypurine tract; BSA, bovine serum albumin; PNK, T4 polynucleotide kinase; DTT, dithiothreitol; EDTA, ethylenediaminetetraacetic acid.

10.1021/bi051770w CCC: $33.50
Published on Web 05/24/2006

mM) is used (*24*, *32*). Also, site-specific photo-cross-linking has shown that close contacts occur between amino acids at the far C-terminus of RNase H (near the αE′ helix) and the primer-template. Interestingly, there were subtle differences in the contacts for the RNA−DNA vs DNA−DNA substrates (*26*). Overall, the results show that contacts with the primer-template outside the pol region and at the RNase H active site can affect binding and polymerase catalysis, although they do not directly show that binding affinity under optimal conditions is significantly affected.

We set out to determine the contributions of the RT domains to binding RNA−DNA vs DNA−DNA. Binding of RT to unique chimeric substrates that positioned RNA−DNA or DNA−DNA near the different domains was measured. Results showed that the severalfold tighter binding to RNA−DNA was determined mostly by contacts between this substrate occurring near the pol active site, and only a small RNA−DNA hybrid region was required for tight binding.

MATERIALS AND METHODS

Materials. Custom primers used in all experiments were purchased from Integrated DNA Technologies. T4 polynucleotide kinase (PNK) and bovine serum albumin (BSA) were from New England Biolabs. PCR grade dNTPs were from Roche Applied Sciences. Radiolabeled nucleotides were from GE Healthcare (formerly Amersham Biosciences). RNase H minus HIV-RT E478Q (glutamic acid to glutamine) and wild-type HIV-RT from strain HXB-2 were a kind gift from Dr. Stuart Le Grice (NIH HIV Drug Resistance Program, Frederick, MD). All other chemicals or enzymes used were from Fisher Scientific or Sigma-Aldrich.

Preparation of Radiolabled Primers. Twenty-five picomoles of primer DNA was 5′-^{32}P-end-labeled using PNK. The labeling reaction was done at 37 °C for 30 min using the manufacturer's protocol. The PNK was heat inactivated by incubating the reaction at 65 °C for 15 min. The DNA was centrifuged on a Sephadex G-25 column to remove excess radiolabeled nucleotide.

Preparation of Hybrids for Off-Rate Determinations. Hybrids were prepared by mixing 0.18 pmol of 5′-^{32}P-labeled DNA primer (23, 28, 33, 38, or 43 nucleotides) and 0.12 pmol of template [D50, R50, 5′-D20R30, 5′-R20D30, or 5′-D15R5D30 (see Figure 1)] in 10 μL of 50 mM Tris-HCl (pH 8.0), 1 mM DTT, 80 mM KCl, and 0.1 mM EDTA (pH = 8). The reaction was then slowly cooled from 70 °C to room temperature and immediately placed on ice.

Determination of Dissociation Rate Constants (k_{off}) by Nucleotide Incorporation. HIV-RT HXB-2 (E478Q or wild type, 37.5 nM) was preequilibrated with 5′-end-labeled primer-template (5 nM template, 7.5 nM primer) for 3 min at 37 °C in 40 μL of 50 mM Tris-HCl (pH 8.0), 0.1 mM EDTA (pH 8.0), 80 mM KCl, 6 mM $MgCl_2$, 1 mM DTT, and 0.1 μg/μL BSA. In some experiments with wild-type RT the $MgCl_2$ was omitted, KCl was at 5 mM, and 0.1 mM EDTA (pH = 8) was included. After preequilibration, 10−20 μg (as required for effective trapping of the enzyme over the reaction time course) of poly(rA)−oligo(dT)$_{20}$ in 10 μL of the above buffer was added to the reactions. The poly(rA)−oligo(dT)$_{20}$ was used as a "trap" to bind and sequester RT molecules that dissociated from substrates (*33*). Poly(rA)−oligo(dT)$_{20}$ used in the reactions was prepared by mixing oligo(dT)$_{20}$ with poly(rA) at a 1:8 ratio (w/w), respectively, in 10 mM Tris-HCl (pH 8.0) and 0.1 mM EDTA (pH 8.0). The mixture was incubated for 10 min at 37 °C. After trap addition, 5 μL aliquots were removed at 1, 2, 4, 8, and 16 min (unless otherwise stated) and placed in a tube containing 1 μL of dNTP mix (600 μM dNTPs in the above buffer, including 36 mM $MgCl_2$ for reactions without $MgCl_2$ in the preincubation). Tubes were incubated for 3 min at room temperature and then terminated by addition of 6 μL of 2× sample buffer [90% formamide, 20 mM EDTA (pH 8.0), 0.1% xylene cyanol, 0.1% bromophenol blue]. A $t = 0$ sample was prepared by adding 4 μL of the preequilibration mix to a tube containing 1 μL each of trap mix and dNTP mix and incubating as above. Since the dissociation of the enzyme−nucleic acid substrate complexes is slow relative to the rate of polymerization (*34*, *35*), the amount of synthesis is proportional to the amount of bound RT at the initiation of the reactions. Samples were loaded onto a 10% polyacrylamide/7 M urea sequencing gel and subjected to electrophoresis as described (*36*). Quantification of extended primer was accomplished by phosphorimager analysis of dried gels, using a FX Pro phosphoimager from Bio-Rad. The dissociation rate constants (k_{off}) were determined by constructing a graph of the amount of extended primer vs time. A nonlinear least-squares fit of the data to an equation for single-exponential decay [$f(x) = ae^{-bx}$, where a is the y intercept at time 0 and b is the dissociation rate] was used to graph the data using Sigma Plot (Jandel Corp.). The time 0 point was not included in the calculations. The weaker binding substrates generally showed a disproportionately large decrease in extension between $t = 0$ and the first time point, resulting in a poorer fit of the data to the above equation. Removing time 0 improved the fits. This phenomenon could result from RT enzymes in the open as opposed to closed conformation, dissociating rapidly in the presence of the trap (*37*, *38*).

Mapping of 5′-D20R30-3′ Bound to Primers of Various Lengths. Mapping was performed using a previously described method (*15*). Hybrids between 5′-^{32}P-labeled template 5′-D20R30-3′ and primers P23, P28, P33, P38, and P43 were prepared as described above. The template was labeled using PNK as described above. Reaction mixtures including primer-template (5 nM template, 7.5 nM primer), 50 mM Tris-HCl (pH 8.0), 0.1 mM EDTA (pH 8.0), 80 mM KCl, 6 mM $MgCl_2$, 1 mM DTT, and 0.1 μg/μL BSA were preequilibrated in the presence or absence of E478Q (37.5 nM final concentration when present) in a total volume of 10.5 μL for 3 min at 37 °C. *Escherichia coli* RNase H [2 μL at 0.25 unit/μL in 50 mM Tris-HCl (pH 8.0), 0.1 mM EDTA (pH 8.0), 80 mM KCl, and 1 mM DTT] was added, and 4 μL aliquots were removed and placed into an equal volume of 2× sample buffer after 1, 2, and 4 min. Samples were loaded onto a 10% polyacrylamide/7 M urea sequencing gel and subjected to electrophoresis (*36*).

Cleavage Assays with HIV-RT and E. coli RNase H. Primer-template [5 nM template, 7.5 nM primer (either P33 or P38)], 5′-end-labeled on the template strand, was preincubated for 3 min at 37 °C in 10.5 μL of 50 mM Tris-HCl (pH 8.0), 0.1 mM EDTA (pH 8.0), 80 mM KCl, 7.1 mM $MgCl_2$, 1 mM DTT, and 0.12 μg/μL BSA. Two microliters of HIV-RT HXB-2 (37.5 nM final concentration in reactions)

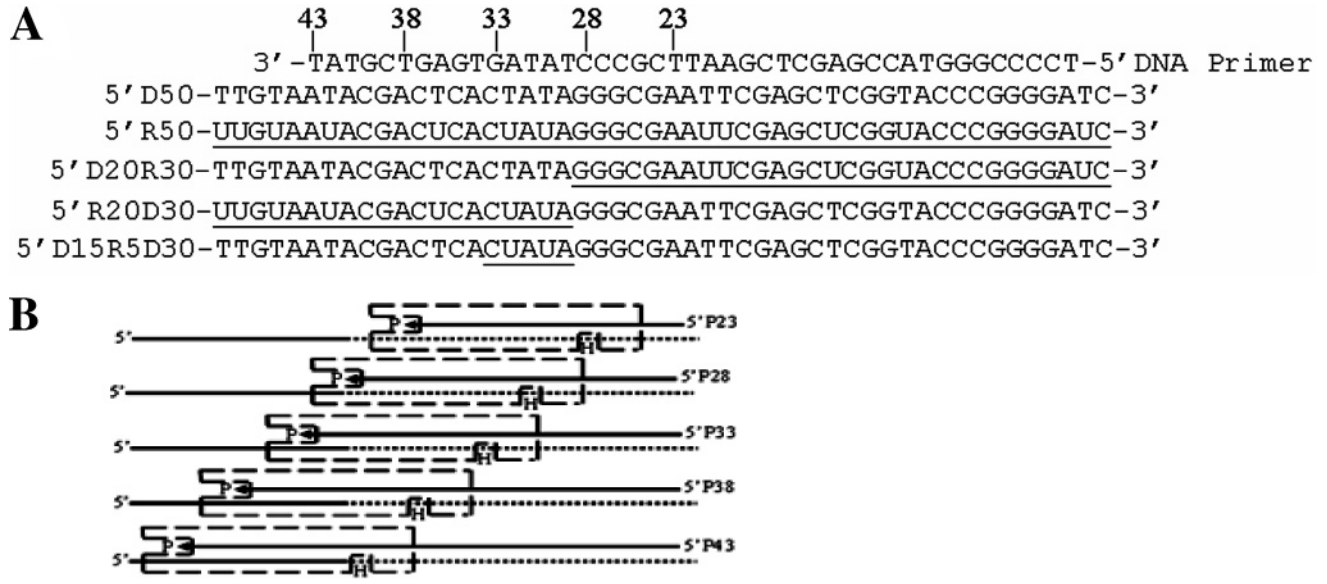

FIGURE 1: Sequence and configuration of nucleic acid substrates. (A) The sequences of the primer (top stand) and template strands are shown. Five different DNA primers that shared a common 5′ end were used. Their lengths were 23, 28, 33, 38, and 43 nts as marked above the primer strand. The primer is placed over the complementary bases of the various template strands. The templates were all 50 nts and consisted of either homogeneous DNA or RNA or chimeras with both DNA and RNA. RNA nts are underlined on the templates. Substrates were named on the basis of the primer and template used with the following nomenclature as an example: P33-D20R30. This substrate had the 33 nt DNA primer hybridized to the 5′-D20R30-3′ template strand. (B) Shown is the presumed orientation of reverse transcriptase on substrates with P23, P28, P33, P38, and P43 bound to 5′-D20R30-3′. The polymerase active site (P) is positioned at the 3′ recessed primer terminus while the RNase H active site (H) is approximately 18 nts in back over the duplex region of the substrate. The RNA and DNA portions of the template strand are in dotted and solid lines, respectively.

or *E. coli* RNase H (0.5 unit) in 50 mM Tris-HCl (pH 8.0), 0.1 mM EDTA (pH 8.0), 80 mM KCl, and 1 mM DTT was added, and reactions were continued for 5 s or 15 min. Reactions were terminated with 12.5 μL of 2× sample buffer and electrophoresed on a 12% denaturing polyacrylamide gel as described above. Base hydrolysis ladders for templates R50 and 5′-D20R30-3′ were prepared by incubating, in 5 μL, 2 pmol of 5′-^{32}P-end-labeled template at 65 °C for 30 s in 0.1 M NaOH and terminating the reactions with 1 μL of 0.5 M HCl. Fourteen microliters of water and 20 μL of 2× sample buffer were then added. RNase T1 hydrolysis was performed using 1 or 5 units of T1 RNase and 2 pmol of template in 20 μL of 50 mM Tris-HCl (pH = 7.5), 4 mM EDTA (pH = 8), 2 pmol/μL tRNA, and 3.5 M urea for 15 min at 37 °C. Twenty microliters of 2× sample buffer was then added.

RESULTS

Rationale for Substrate Design and Assay. Shown in Figure 1A are sequences of different substrates used in binding assays. Five different DNA primers with common 5′ ends ranging from 23 to 43 nts were 5′-^{32}P-end-labeled and hybridized to one of five template strands. The template strands were 50 nts long and were composed of DNA, RNA, or combinations of these as indicated. Hybrid substrates are referred to in the text with the primer name followed by the template name (for example, P33-R20D30). Binding of the pol domain of RT to the 3′ end of the primer would position RT at various locations along the template strand. This is illustrated in Figure 1B for the various primers bound to 5′-D20R30-3′. Note that some primers position both the pol and RNase H sites over the RNA−DNA hybrid while others position pol over DNA−DNA and RNase H over RNA−DNA. This allowed a comparison of the contributions of the domains to observed tight binding of RNA−DNA vs DNA−DNA. To determine the stability of the binding between RT and substrates, dissociation rate constants (k_{off}) were determined. This was done by prebinding RT to the substrate and then adding excess poly(rA)−oligo(dT) as a trap to sequester RT that did not bind or dissociated from the substrate. At various times after trap addition, dNTPs were added to allow extension of the primers on substrates that RT was bound to. Plots were constructed and used to determine off-rates as described in the Materials and Methods section.

For most experiments, RNase H minus mutant HIV-RTE478Q was used instead of wild-type RT. Under the conditions used, this enzyme binds nearly identically in comparison to wild-type RT (*24*). It also has DNA synthetic properties that essentially mimic the wild type and has been used for several studies requiring DNA polymerase activity in the absence of RNase H (*39*−*42*) and also crystal structures (*21*). The reason for using the mutant was so Mg^{2+} could be included in the prebinding step without resulting in degradation of the substrate. Those substrates with RNA−DNA hybrid regions would presumably be cleaved by RNase H with wild-type RT. Although Mg^{2+} could have been omitted, it has been shown to greatly affect the stability of RT binding to substrates, typically resulting in severalfold slower dissociation (*13*, *24*). Binding measurements with Mg^{2+} are therefore more representative of physiological conditions. For some substrates assays were also conducted with Mg^{2+} and wild-type RT, and no significant difference was observed (see below). This indicates that E478Q is a good model for binding of wild-type RT to the substrates (see Discussion).

Comparison of k_{off} Values Using the Homogeneous RNA and DNA Templates Reveals Some General Trends with the Substrates. Shown in panels A and B of Figure 2 are

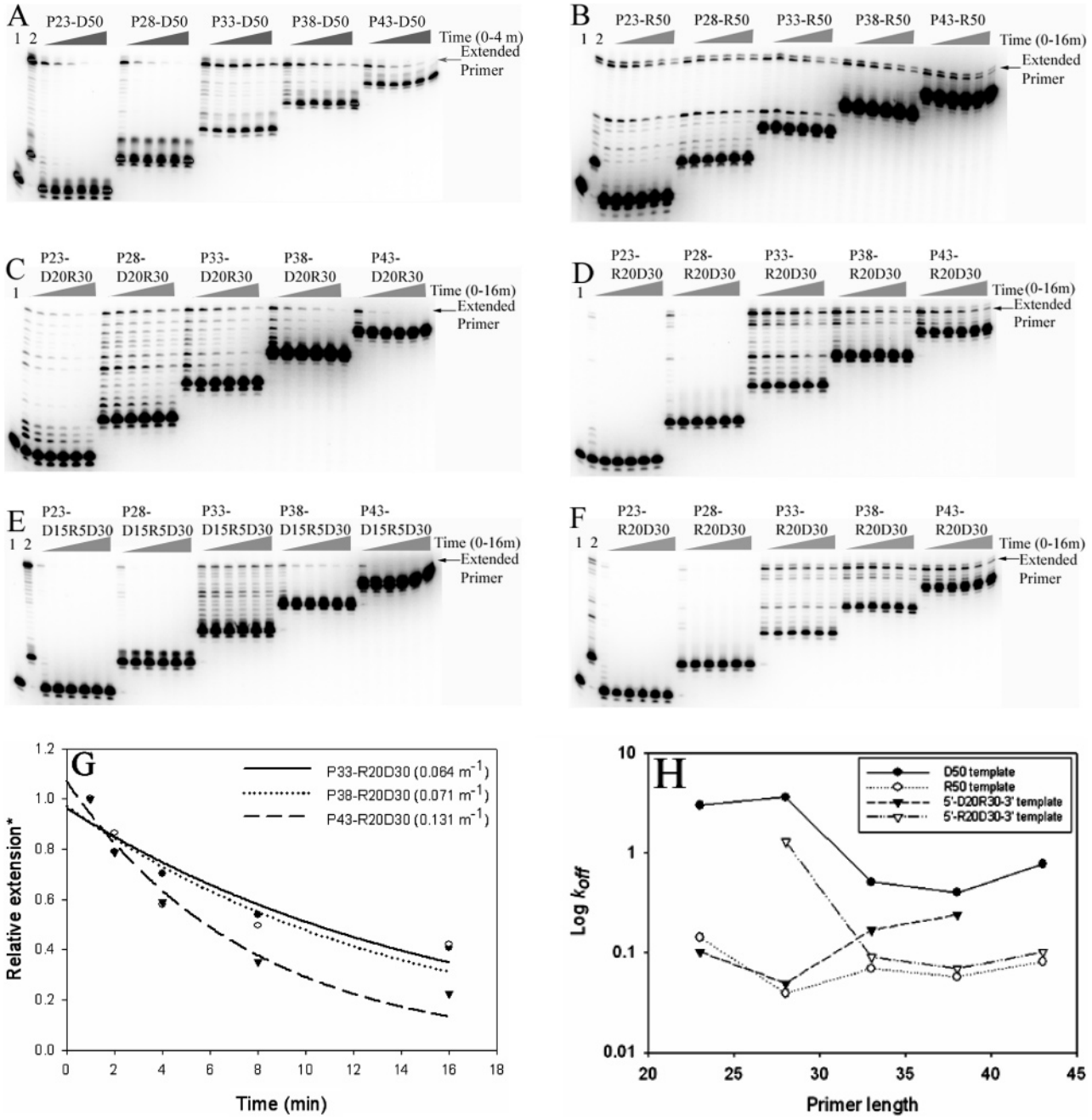

FIGURE 2: (A−H) Autoradiograms and graphs for dissociation rate constants (k_{off}). Panels A (D50 template), B (R50 template), C (5′-D20R30-3′), D (5′-R20D30-3′), E (5′-D15R5D30-3′), and F (5′-R20D30-3′ with wild-type RT) show autoradiograms from typical experiments used to calculate reverse transcriptase k_{off} values for the template strand bound to P23, P28, P33, P38, or P43. The substrate name is written above each set of assays. Time points from left to right for each set were 0, 15 s, 30 s, 1 min, 2 min, and 4 min in panel A and 0, 1 min, 2 min, 4 min, 8 min, and 16 min in panels B−F. All experiments were conducted with RT E478Q except for panel F which used wild-type RT. The position of the fully extended primer is indicated on each panel. Lane 1 shows a control reaction to test the effectiveness of the poly(rA)−oligo(dT) trap (see Materials and Methods). In this reaction the enzyme was mixed with the trap, and the mixture was added to one of the substrates in the presence of dNTPs and divalent cation and incubated for a time equal to the longest time point on the gel. Lane 2 shows a full extension control in which enzyme was incubated with one of the substrates as in the trap control reaction except the trap was omitted to allow all of the bound primer to be extended. The k_{off} values for the experiment shown in panel F for P33-R20D30, P38-R20D30, and P43-R20D30 were 0.031, 0.050, and 0.078 min^{-1}, respectively. Values for experiments with E478Q are reported in Table 1. (G) A typical graph generated using the 5-R20D30-3′ template bound to the P33, P38, or P43 primer is shown. Each line is a fit of the data to an equation for single-exponential decay [$f(x) = ae^{-bx}$, where a is the y intercept at time 0 and b is the dissociation rate constant (k_{off})] that was used to determine k_{off} (see Materials and Methods). Values of k_{off} are listed on the key for the various substrates in this particular experiment. For comparison purposes on this graph the first time point for each line was set equal to 1, and all other time points are relative to this value. (H) Graph of log k_{off} vs primer length for template D50, R50, 5′-D20R30-3′, and 5′-R20D30-3′. The average k_{off} values from Table 1 were used to construct the plot. The x axis is a plot of primer length.

autoradiograms from experiments with P23, P28, P33, P38, and P43 primers bound to the 50 base DNA (D50) or RNA (R50) templates, respectively. A typical graph used to determine k_{off} values is shown in Figure 2G (using the 5′-R20D30-3′ template). Table 1 shows off-rates for all substrates used in this paper. Experiments were repeated two

Table 1: Dissociation Rate Constants (k_{off}) Determined for the Various Primer-Templates

	template[a]				
primer/enzyme[a]	D50	R50	5′-D20R30-3′	5′-R20D30-3′	5′-D15R5D30-3′
P23/E478Q	2.98 ± 0.40[b]	0.142 ± 0.053	0.102 ± 0.030	ND	ND
P28/E478Q	3.59 ± 0.13	0.039 ± 0.018	0.049 ± 0.008	1.29 ± 0.17	ND
P33/E478Q	0.508 ± 0.322	0.069 ± 0.004	0.168 ± 0.092	0.070 ± 0.007	0.027 ± 0.002
P38/E478Q	0.399 ± 0.058	0.057 ± 0.011	0.238 ± 0.028	0.069 ± 0.004	ND
P43/E478Q	0.771 ± 0.329	0.081 ± 0.016	ND	0.101 ± 0.042	ND
P28/WT-Mg[c]	0.347 ± 0.012	VS	0.020 ± 0.002	0.724 ± 0.221	ND
P33/WT-Mg	0.079 ± 0.030	VS	0.166 ± 0.059	VS	ND

[a] Primers and templates are as described in Figure 1. E478Q, HIV-RT mutant without RNase H activity; WT, wild-type RT. [b] k_{off} values were determined as described in Materials and Methods. Results are an average of two to three experiments ± standard deviations, and the units are in min^{-1}. ND, not determined; VS, very stable binding was observed with little or no decay over the 16 min assay time. [c] Assays without Mg^{2+} in the preincubation step were conducted using 5 mM KCl instead of the standard 80 mM.

to three times, and values are expressed as averages ± standard deviations. In some cases dissociation rates were not determined (ND). As expected, these experiments showed that RT bound RNA−DNA much tighter (about 1 order of magnitude) than DNA−DNA [note that the time course in Figure 2A (DNA template) was over 4 min while it was over 16 min for other templates]. Both D50 and R50 substrates showed a more rapid dissociation with the short 23 nt primer. With both this primer and P28 dissociation was very rapid using the DNA template. Dissociation with the longest primer (P43) was also more rapid for both templates. These observations are probably due to a combination of things including "end effects" and variations due to different sequences being bound at the primer 3′ termini. The end effects result from the particular primer positioning RT near the termini of the substrate. It has been shown that this can destabilize RT−substrate binding (*32*). Although RT clearly binds with less stability to short primers, all of the primers used here were long enough such that this should not have had a dramatic effect (*43*). However, some difference based on primer length might still be expected for primers such as P23 for which the primer is shorter than the approximately 24−25 nt footprint RT makes on the primer strand of primer-templates (*41*). With respect to differences in the sequences that each primer binds, relatively little is known about how primer-template sequences can affect binding. Recent results from our laboratory have indicated that some specific DNA−DNA sequences can bind RT with much greater stability than others (unpublished data). Given this, it would not be surprising if some of the observed variations resulted from the different sequences near the primer 3′ terminus. Finally, the shorter primers expose more of the template 5′ nucleotides, making it easier for these bases to form secondary structures or "dimerize" with other substrates. This could potentially affect RT binding. The 25 nts exposed when P23 was used were not predicted to form a stable structure with folding programs, but potential dimer formation was predicted.

Comparison of k_{off} with Chimeric Templates Indicates That Binding of RNA−DNA near the Polymerase but Not the RNase H Domain Is Responsible for the Tight Binding to RNA−DNA Hybrids. Shown in panels C and D of Figure 2 are autoradiograms from experiments with P23, P28, P33, P38, and P43 bound to 5′-D20R30-3′ (Figure 2C) or 5′-R20D30-3′ (Figure 2D). Figure 2H shows a plot of k_{off} vs primer length with E478Q RT for all templates used in the assays except 5′-D15R5D30-3′. Note that a log scale is used for k_{off} values due to the large differences. The chimeric templates show essentially the reverse pattern for binding stability. For 5′-D20R30-3′ shorter primers showed the most stable binding, especially P28, while binding was relatively weak with P38 and P43. For 5′-R20D30-3′, dissociation with both P23 and P28 was very fast while the tightest binding was observed with P33 and P38. Primer P28 is notable because it presumably positions the RT pol active site right at the RNA−DNA junction of both 5′-R20D30-3′ and 5′-D20R30-3′. Therefore, P28-D20R30 positions the active site and surrounding protein domain (moving from the pol active site toward the RNase H domain) such that both the polymerase and RNase H domains are positioned over RNA−DNA (see Figure 1B). Primer P33 begins to move the pol domain over DNA−DNA, and P38 and P43 would position even more of this domain over DNA−DNA. For 5′-R20D30-3′, both domains are bound to DNA−DNA with P28, while five base pairs of the RNA−DNA hybrid are presumably bound in the pol domain with P33 and 10 with P38. The transition observed with this template bound to P28 or P33 is remarkable in that the off-rate goes from very fast (similar to P28-D50) to very slow (essentially equivalent to P33-R50), an order of magnitude difference (Figure 4 and Table 1). For P28-D20R30 and P33-D20R30 the change is in the opposite direction, going from slow to fast with P28 and P33, respectively. In this case the magnitude of the change is smaller although P33-D20R30 clearly shows faster dissociation. P28-D20R30 binds equivalently to P28-R50. P38-D20R30 binds similarly to P38-D50. Overall results show that positioning RT's polymerase domain near RNA−DNA greatly stabilizes binding, even if only a small RNA−DNA patch is present (five base pairs with P33-R20D30). Also, the substrate with only a 5 base pair RNA−DNA hybrid region positioned near the pol active site (P33-R20D30) bound as stably as the same primer hybridized to a homogeneous RNA and forming a 33 base pair RNA−DNA hybrid that would span the entire enzyme (P33-R50). Those substrates that did not have RNA−DNA positioned at the pol site bound much less stably, even if much of the enzyme was still bound to RNA−DNA (compare P28-D20R30 to P33- and P38-D20R30).

A Template Strand with Only 5 RNA Nucleotides Binds Like a Complete 50 Base RNA Template When the 5 Nucleotides Are Positioned near the Polymerase Active Site of RT. To determine if a small RNA−DNA hybrid region was sufficient for tight binding, a template that had only 5 nts of RNA was designed. Template 5′-D15R5D30-3′ is

similar to 5′-R20D30-3′ except that the 15 RNA nts at the 5′ end were replaced with DNA. Primers P23, P28, P33, P38, and P43 were hybridized to the template, and off-rates were determined. An autoradiogram is shown in Figure 2E, and the k_{off} value for the P33 hybrid is shown in Table 1. The off-rates for other primers could not be determined using the time points shown because dissociation was very rapid. Only P33-D15R5D30 showed tight binding to RT. This substrate positions the pol active site over a 5 nt RNA−DNA hybrid. The off-rate (0.027 min^{-1}) for the substrate is actually even lower than the values for P33-R50 (0.069 min^{-1}) or P33-R20D30 (0.070 min^{-1}), indicating somewhat tighter binding. The results show that only a 5 nt RNA−DNA hybrid region is required for binding equivalent to a large RNA−DNA hybrid. Note that the off-rate is clearly much faster for P38-D15R5D30. In this substrate the 5 nt RNA−DNA hybrid region is still presumably bound near the pol domain but has been shifted away from the polymerase active site toward the RNase H domain. The significantly weaker binding of this substrate to RT brings out the importance for the RNA−DNA region being located at the pol active site.

Wild-Type RT and HIV-RT E478Q Show Comparable Binding with the Substrates. For the reasons noted above, HIV-RT E478Q was used for the binding assays. To compare binding of this enzyme to wild type on the various substrates, assays were performed with D50, 5′-D15R5D30-3′, and 5′-R20D30-3′. Because cleavage of the RNA was observed during preincubation when using the R50 and 5′-D20R30-3′ templates with wild-type enzyme (see below), accurate dissociation rates could not be measured for these substrates with Mg^{2+}. An off-rate assay using wild-type RT with P23, P28, P33, P38, and P43 bound to 5′-R20D30-3′ is shown in Figure 2F. The pattern is essentially the same as was observed with E478Q on the same template (see Figure 2D). Reverse transcriptase bound most stably when primers P33 or P38 were used, and binding was weak with P23 and P28. No significant difference was observed between the binding of wild type and E478Q to the 50 nt DNA template or 5′-D15R5D30-3′ (data not shown).

To further substantiate results with E478Q, assays with wild-type RT were also conducted with various templates in the absence of Mg^{2+}. This allowed analysis of those templates for which Mg^{2+} could not be included in the preincubation step (see above). Since this modification greatly weakens RT binding (see above), 5 mM KCl was used rather than 80 mM in order to enhance binding enough to obtain an accurate off-rate. Binding of P28 and P33 to D50, R50, 5′-D20R30-3′, and 5′-R20D30-3′ was measured. Consistent with the above results, RT bound much more tightly when RNA−DNA was at the pol active site. Dissociation over 16 min under these conditions was too slow to accurately measure for several substrates (VS) and also slow for P28-D20R30 (k_{off} 0.020 min^{-1}; see Table 1, WT RT-Mg^{2+}). For those substrates with DNA−DNA at the pol site binding was much weaker. The P33-D20R30 substrate, which positions 5 base pairs of DNA−DNA at the pol site while the rest of the enzyme is occupied by RNA−DNA, bound somewhat less stably than the same primer hybridized to DNA (k_{off} 0.166 vs 0.079 min^{-1} for P33-D20R30 and P33-D50, respectively). This result suggests that RNA−DNA occupying regions of the enzyme other than the immediate pol active site has no significant stabilizing effect.

Physical Mapping Indicates That RT Binds near the 3′ Primer Terminus on the 5′-D20R30-3′ Template. As was noted in the introduction, the pol domain of RT binds near the 3′ recessed terminus on DNA primers and the 5′ terminus on non-ppt RNA primers. The unique nature of the chimeric templates used here could affect where RT preferentially binds. The fact that primers were extended in these assays indicates RT can bind at the primer's 3′ terminus; however, it is still possible that only a fraction of the protein binds in this orientation while most binds in a nonproductive orientation. To determine the location of RT on chimeric templates, a physical mapping technique previously used to map the position of RT on RNA primers was used (*15*). E478Q was prebound to the various primer-templates using the 5′-D20R30-3′ template which was 5′-^{32}P-end-labeled. *E. coli* RNase H was then added, and samples were digested for 1, 2, or 4 min. Control reactions were performed in the absence of RT. Any portion of the RNA−DNA hybrid that is covered by RT will be protected from degradation with RNase H. If RT binds to the 3′ primer terminus, then the smaller primers (P23 and P28) should position it essentially over most of the RNA−DNA. Longer primers will expose more of the hybrid and should result in shorter degradation products with *E. coli* RNase H (see Figure 3B). The autoradiogram in Figure 3A shows an experiment generally consistent with RT binding to the primer terminus. With primer P23 in the presence of E478Q, template strands shortened by 1−9 nts (41−49 nt products, marked by a vertical line on the gel under P23-D20R30) were evident, and a relatively larger portion of the template was not cleaved over the 4 min time course. A group of cleaved templates shortened by 2−7 nts (43−48 nts) appeared with P28. With P33 and P38 the major group of protected products became progressively shorter, consistent with the scenario proposed above. With P43 some protection was observed for products of 29 and 30 nts, but there was also some clear protection for longer products, closely resembling the pattern with P23. This was also seen to some extent with P38 although the vast majority of protected products with this primer were in the 32−36 nt range. Like P23, full-length templates were also more resistant to cleavage with P43. The likely explanation is that the polymerase can bind stably at more than one place on the template with P43. Some bind near the primer terminus, resulting in the shorter protected products (29−30 nts), and some bind at the other end of the template in the RNA−DNA hybrid region, resulting in the longer protected products.

RT Cannot Cleave 5′-D15R5D20-3′ or 5′-R20D30-3′ Bound to P33 or P38 despite Binding Tightly to These Substrates, and Cleavage of 5′-D20R30-3′ and R50 Bound to P33 or P38 Results in the Same Cleavage Products. Cleavage assays with wild-type RT and *E. coli* RNase H were performed on some of the substrates, and the results are shown in Figure 4. Templates 5′-D20R30-3′, 5′-R20D30-3′, and 5′-D15R5D30-3′ bound to P33 or P38 were compared to R50 bound to the same primers. Assays of 5 s and 15 min were conducted with R50 and 5′-D20R30-3′. The 5 s assays allowed observation of early cleavages. Results for these templates were consistent with early cleavages of both resulting in mostly 31−34 and 26−28 nucleotide long products when bound to P33 and P38, respectively. These

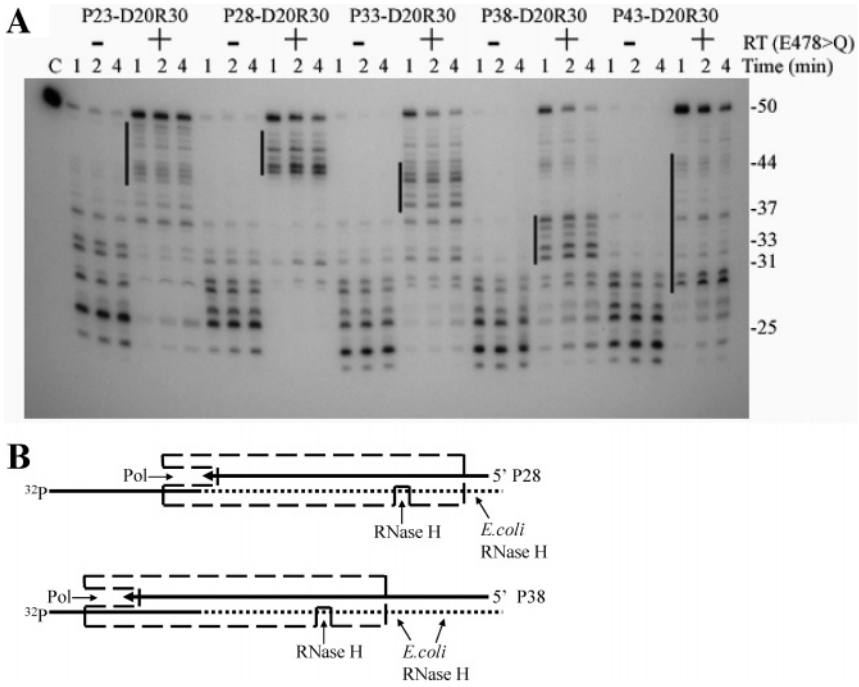

FIGURE 3: (A and B) Mapping of the position of HIV-RT on the 5′-D20R30-3′ template bound to P23, P28, P33, P38, or P43 primers. An autoradiogram from a typical mapping experiment is shown in panel A while a schematic illustration of the experiment is shown in panel B. The substrate (5′-^{32}P-labeled on the template strand) was preincubated in the presence (+) or absence (−) of RT E478Q, then *E. coli* RNase H was added, and incubation was continued to 1, 2, or 4 min as indicated. The name of each substrate is written above the assay lanes. A vertical line marking the positions of the most prevalent products that were protected by E478Q from cleavage by *E. coli* RNase H is shown for each substrate. A size marker is shown on the far right and indicates the size of products in nucleotides. Positions indicated were based on a G-ladder constructed by digesting the template strand with T1 RNase (data not shown). Lane C: Undigested template starting material. (B) A schematic diagram illustrating why shorter protected products are observed with longer primer strands is shown. Primers P28 or P38 are shown bound to the 5′-D20R30-3′ template (DNA, solid line; RNA, dotted line) that is labeled at the 5′ end with ^{32}P. An RT molecule is shown oriented on each substrate, illustrating that P38 exposes more RNA−DNA hybrid to cleavage than P28.

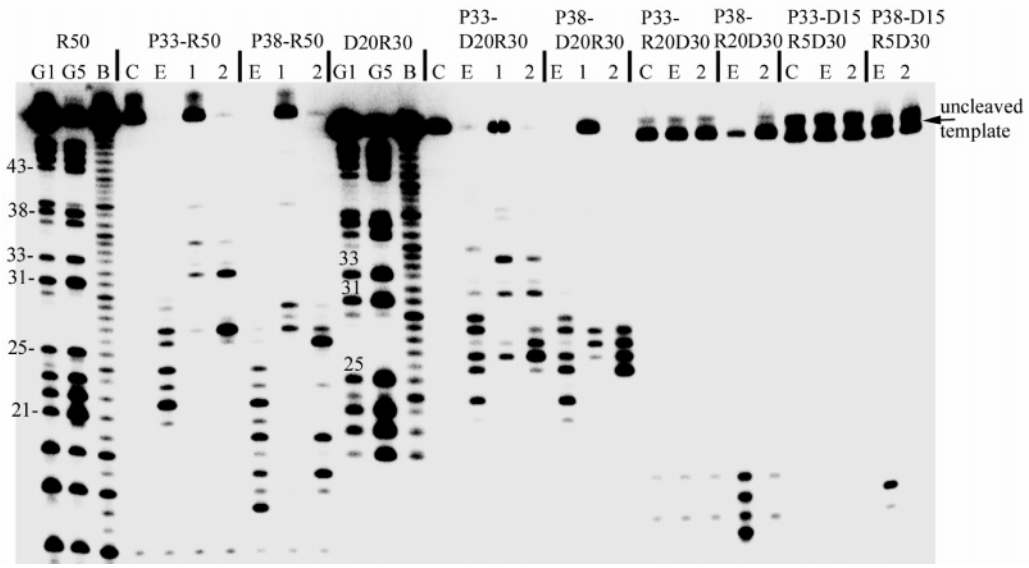

FIGURE 4: Cleavage of substrates with wild-type HIV-RT. Shown is an autoradiogram of 5′-^{32}P-end-labeled templates R50, 5′-D20R30-3′, 5′-R20D30-3′, and 5′-D15R5D30-3′ bound to P33 or P38 and cleaved with wild-type HIV-RT (lanes labeled 1 and 2 are 5 s and 15 min cleavage reactions, respectively) or *E. coli* RNase H (lane E, 15 min cleavage reaction). Lanes labeled C are control reactions incubated for 15 min without enzyme. Size markers (in nucleotides) for the R50 and 5′-D20R30-3′ templates were produced by base hydrolysis (B) or digestion with one (G1) or five (G5) units of T1 RNase as described in Materials and Methods. T1 cleaves after G residues in the RNA. R50 and 5′-D20R30-3′ have the same RNA sequence for the 30 3′ nucleotides so they show common cleavages. Those for the latter are shifted downward slightly because of faster migration caused by the DNA portion of the template. The position of uncleaved template is also indicated.

sizes correspond to cleavages 16−19 and 16−18 nucleotides behind the 3′ primer terminus for P33 and P38, respectively. The numbers are in good agreement with experiments that show the RNase H active site about 18 nucleotides removed from the pol site (*4*−*10*). The results further support RT binding at the primer terminus on the chimera. The identical cleavage positions also indicate that the DNA−RNA junction on the 5′-D20R30-3′ substrate does not result in a substantial

change in the trajectory of the primer-template during binding to RT (see Discussion).

Experiments with 5′-R20D30-3′ and 5′-D15R5D30-3′ bound to P33 and P38 were conducted for 15 min only, and in both cases no cleavage was observed with RT. Note that RT binds tightly to P33-R20D30 and P38-R20D30 as well as P33-D15R5D30 (see Table 1). Interestingly, *E. coli* RNase H cleaved these templates only when bound to P38, and cleavage of P38-D15R5D30 was weak. The results indicate that these substrates probably trap RT in a configuration where the RNA−DNA hybrid regions of the substrates are not bound near the RNase H domain, even transiently.

DISCUSSION

Our goal in this study was to understand what determines RT's strong preference for stable binding to RNA−DNA vs DNA−DNA, in particular, if contacts in the polymerase and RNase H domains or both are required. Results showed that only a small patch of RNA−DNA was required for tight binding, providing that it was positioned in the polymerase domain near the primer terminus. Surprisingly, RT dissociated from a substrate with a 5 nt RNA−DNA hybrid region (P33-D15R5D30) positioned near the pol active site at a rate comparable to a 33 nt RNA−DNA hybrid spanning the entire enzyme (P33-R50) (see Table 1).

Results with the 5′-R20D30-3′ and 5′-D15R5D30-3′ templates indicated that only 5 base pairs of RNA−DNA hybrid at the primer terminus are necessary to achieve a binding stability equivalent to a complete RNA−DNA hybrid that spans both enzyme domains (see Figure 2D,E and Table 1; compare P33-R20D30 and P33-D15R5D30 to P33-R50). Assuming that RT's pol active site is bound to the 3′ primer terminus on P33-R20D30 and P33-D15R5D30, the 5 base pair RNA−DNA hybrid portion of the substrate would be in immediate contact with the β12−β13 hairpin region in the palm subdomain known as the "primer grip". A portion of the hybrid would also extend back near helix αH located on the thumb. This region has been implicated in stabilizing primer-template binding while the primer grip is important for stable binding and proper orientation of the primer for catalysis (reviewed in ref *19*). As was indicated in the introduction, crystal structures of RT with DNA−DNA or RNA−DNA hybrids show several additional interactions with RNA−DNA. Since RNA−DNA and DNA−DNA hybrids bound to RT follow the same trajectory and have the same bend angle (*21*, *22*, *44*), differential binding likely results from additional interactions with amino acids. Most notable are 11 additional predicted interactions with 2−hydroxyls of RNA. Five of these occur within the first 5 nts of the primer terminus: tryptophan 153 and lysine 154 to position 1 (template base bound to primer 3′ terminal base; subsequent numbering in the text is 5′−3′ on the template moving toward the RNase H domain) and glutamic acid 89, glutamine 91, and isoleucine 94 to positions 2, 3, and 4, respectively (*22*). Our results suggest that interactions of RNA−DNA hybrids with these amino acids are most responsible for tight binding. Note that this does not mean that the additional interactions have no effect on stabilizing binding, but if they do, it is relatively small (see below).

The current results suggest that additional contacts with RNA outside the first 5 base pairs of the pol active site have at most a small effect on stabilizing substrate binding. There are six such interactions with 2′-hydroxyls including three near the RNase H domain: glutamine 475 to nucleotide position 18 and two with arginine 448 to positions 19 and 20. Three others occur closer to the pol active site: asparagine 265 and lysine 353 with position 6 and arginine 284 with position 8. Our current hypothesis is that these interactions may serve to correctly orient and position the substrate for catalysis at the RNase H active site. Two mutations [glutamine 475 (Q475A) and arginine 448 (R448A)] in amino acids that interact with 2′-hydroxyls outside the pol region have been tested. Mutant Q475A showed a reduction in virus yields and some alterations in RNase H cleavage specificity while R448A had no effect on virus titer in a single round of infection (*30*). Since Q475 is part of the RNase H primer grip domain that is known to be important in positioning the primer-template (both DNA−DNA and RNA−DNA) for nucleotide addition and RNase H catalysis (*29*−*31*), the observed mutant phenotype did not necessarily result from effects on RNA binding. The wild-type phenotype of R448A might suggest that this residue's interactions with RNA 2′-hydroxyls are inconsequential. However, the mutant was only analyzed for virus titer in a single cycle assay so a subtle defect may not have been observed. Analysis of additional mutants would be required to clearly understand the role of RNA-specific interactions occurring outside the pol active site region.

Although differential contacts between RNA−DNA and DNA−DNA are likely to substantially underlie tighter binding of RNA−DNA, differences in the structure of the hybrids may also contribute. RNA−DNA adopts an H-form hybrid while DNA−DNA is B-form. Crystallographic analysis of several polymerases including RT indicates that the hybrid region immediately adjacent to the polymerase active site is in an A′-form even for DNA−DNA substrates (*21*, *44*−*46*). The A′-form at the active site and the H-form of RNA−DNA hybrids are not identical (*38*). Still, RNA−DNA may require less distortion than DNA−DNA to conform to an A′-form that is catalytically competent. This could in turn lead to tighter binding. It has also been shown that, upon binding RT, a greater proportion of RNA−DNA as compared to DNA−DNA hybrids rapidly obtain the proper conformation for nucleotide incorporation (*38*). This could be related to RNA−DNA being "closer" to the catalytically competent form but could also result from stronger interactions with ribose nucleotides which could then aid in conforming the substrate for nucleotide incorporation.

Another possible explanation for the chimeric substrates used here binding more tightly than DNA−DNA is that the chimera induces a "kink" or "bend" in the substrate. Crystalline and NMR structural analysis shows that chimeric RNA−DNA hybridized to complementary DNA forms a structure that bends at the RNA−DNA junction (*47*−*53*). On the basis of the approximately 45° bend of the primer-template when bound to RT (*46*), it has been proposed that the bent structure of chimeras may actually help in binding, recognition, and cleavage by RT of chimeric duplexes generated during virus replication (tRNA−DNA and ppt−DNA) (*47*, *49*, *50*). However, results suggest that this did not play a major role for binding of substrates tested here. Off-rates for P28, P33, and P38 bound to 5′-R20D30-3′ were essentially identical to the same primers bound to R50 (Table

1). It seems unlikely that the bend in the substrates would result in off-rates that are nearly identical to those observed for the same primer bound to a homogeneous RNA strand, especially since the different primers would position the bend in different regions of the enzyme. The more likely explanation is that the nature of the RNA−DNA hybrid induces the observed tighter binding. In addition, although the chimeric substrates are likely kinked at the junction, this clearly did not grossly affect the trajectory of the substrates between RT's pol and RNase H active sites. Cleavage analysis showed that 5′-D20R30-3′ bound to P33 and P38 produced essentially the same cleavage pattern as R50 bound to these primers (Figure 4). The most likely explanation is that chimeric substrates are bent and contorted during RT binding in a manner similar to that of nonchimeras.

Although it was necessary to use of E478Q to quantify binding stability (see Results), it could complicate interpretation of some of the results. This is especially notable since the Q475 and R448 interactions with 2′-hydroxyls noted above occur near residue 478. This residue is also important in coordinating divalent cation binding. In addition to the mutant's stronger binding with suboptimal Mg^{2+} noted earlier, others have reported some subtle changes in polymerase activity, though these were only evident on RNA templates and have been proposed to be related to the lack of RNase H activity rather than a direct polymerase effect (*28*, *54*). Still, the mutant clearly cannot completely mimic wild-type interactions near the RNase H site. Therefore, even if interactions in the RNase H active site region contributed to tighter binding for RNA−DNA hybrids, it is possible that this could not be measured with E478Q. Previous binding studies (*24*) and the essentially identical results with wild type and E478Q on templates D50, 5′-R20D30-3′, and 5′-D15R5D30-3′ in the presence of Mg^{2+} suggest that the mutant is a reasonable model for wild-type binding (see Figure 2F and Results). With both wild type and E478Q, positioning of only a 5 base pair RNA−DNA hybrid at the polymerase active site as in P33-R20D30 or P33-D15R5D30 is sufficient for maximal binding with an approximately 10-fold reduction in off-rate compared to binding to D50 (see Table 1). No further gains are achieved by using primers that position a longer RNA−DNA hybrid region over RT. These results clearly implicate interactions with RNA−DNA near the pol site as being pivotal for tight binding. Substrates that positioned the RNA−DNA hybrid outside the pol active site but within the connection and RNase H domains such as P33- and P38-D20R30 (k_{off} 0.168 and 0.238 min^{-1}, respectively) showed low binding compared to those with RNA−DNA bound at the pol site but slightly tighter binding than the P33- and P38-D50 DNA−DNA hybrid (k_{off} 0.508 and 0.399 min^{-1}, respectively). This suggests that these interactions may contribute to binding stability but that their contribution is small and only measurable when binding is relatively weak. However, binding measurements to wild-type RT in the absence of Mg^{2+} with low salt did not bare this out. Substrate P33-D20R30 which positions RNA−DNA throughout most of the enzyme excluding the immediate pol region bound with very low stability (k_{off} 0.166 min^{-1}), showing an increased off-rate relative to the same primer bound to DNA (P33-D50, k_{off} 0.079 min^{-1}). Overall, the results do not support a significant role for the RNase H domain or RNase H primer grip regions of RT in preferentially stabilizing RNA−DNA binding, although a small influence cannot be ruled out.

Finally, it was interesting that RT could not cleave the 5′-R20D30-3′ or 5′-D15R5D30-3′ templates when bound to P33 and P38, despite very tight binding to these substrates (Figure 4). Apparently, the RNase H active site is locked over the DNA−DNA hybrid region by binding of the pol domain to the 3′ primer terminus in the RNA−DNA region. Although it is known that RT can slide along the substrate to perform secondary RNase H cleavages (*55*, *56*), this does not appear to happen on these substrates. Nor does it appear that RT can flip orientations to position the RNase H domain in the RNA−DNA hybrid region. Recent results have suggested that RNA oligonucleotides selected by SELEX (systematic evolution of ligands by exponential enrichment) methods can bind and sequester RT and inhibit replication in cell culture (*57*, *58*). Key to this observation is that the oligo must bind with high affinity and not be degraded by RT. The above substrates, although not optimized for tight binding with respect to sequence, fit these general criteria. We hope this information can be used to help to design nucleic acid-based inhibitors that can bind and sequester RT.

ACKNOWLEDGMENT

We thank Dr. Stuart Le Grice of the NIH HIV Drug Resistance Program for reverse transcriptase.

REFERENCES

1. Hansen, J., Schulze, T., and Moelling, K. (1987) RNase H activity associated with bacterially expressed reverse transcriptase of human T-cell lymphotropic virus III/lymphadenopathy-associated virus, *J. Biol. Chem. 262*, 12393−12396.
2. di Marzo Veronese, F., Copeland, T. D., DeVico, A. L., Rahman, R., Oroszlan, S., Gallo, R. C., and Sarngadharan, M. G. (1986) Characterization of highly immunogenic p66/p51 as the reverse transcriptase of HTLV-III/LAV, *Science 231*, 1289−1291.
3. Starnes, M. C., and Cheng, Y. C. (1989) Human immunodeficiency virus reverse transcriptase-associated RNase H activity, *J. Biol. Chem. 264*, 7073−7077.
4. Furfine, E. S., and Reardon, J. E. (1991) Reverse transcriptase·RNase H from the human immunodeficiency virus. Relationship of the DNA polymerase and RNA hydrolysis activities, *J. Biol. Chem. 266*, 406−412.
5. Wöhrl, B. M., and Moelling, K. (1990) Interaction of HIV-1 ribonuclease H with polypurine tract containing RNA-DNA hybrids, *Biochemistry 29*, 10141−10147.
6. Gopalakrishnan, V., Peliska, J. A., and Benkovic, S. J. (1992) Human immunodeficiency virus type 1 reverse transcriptase: spatial and temporal relationship between the polymerase and RNase H activities, *Proc. Natl. Acad. Sci. U.S.A. 89*, 10763−10767.
7. Fu, T. B., and Taylor, J. (1992) When retroviral reverse transcriptases reach the end of their RNA templates, *J. Virol. 66*, 4271−4278.
8. DeStefano, J. J., Buiser, R. G., Mallaber, L. M., Bambara, R. A., and Fay, P. J. (1991) Human immunodeficiency virus reverse transcriptase displays a partially processive 3′ to 5′ endonuclease activity, *J. Biol. Chem. 266*, 24295−24301.
9. Arnold, E., Jacobo-Molina, A., Nanni, R. G., Williams, R. L., Lu, X., Ding, J., Clark, A. D., Jr., Zhang, A., Ferris, A. L., Clark, P., et al. (1992) Structure of HIV-1 reverse transcriptase/DNA complex at 7 Å resolution showing active site locations, *Nature 357*, 85−89.
10. Kohlstaedt, L. A., Wang, J., Friedman, J. M., Rice, P. A., and Steitz, T. A. (1992) Crystal structure at 3.5 Å resolution of HIV-1 reverse transcriptase complexed with an inhibitor, *Science 256*, 1783−1790.
11. DeStefano, J. J., Buiser, R. G., Mallaber, L. M., Fay, P. J., and Bambara, R. A. (1992) Parameters that influence processive synthesis and site-specific termination by human immunodefi-

ciency virus reverse transcriptase on RNA and DNA templates, *Biochim. Biophys. Acta 1131*, 270−280.
12. Yu, H., and Goodman, M. F. (1992) Comparison of HIV-1 and avian myelblastosis virus reverse transcriptase fidelity on RNA and DNA templates, *J. Biol. Chem. 267*, 10888−10896.
13. DeStefano, J. J., Bambara, R. A., and Fay, P. J. (1993) Parameters that influence the binding of human immunodeficiency virus reverse transcriptase to nucleic acid structures, *Biochemistry 32*, 6908−6915.
14. DeStefano, J. J., Mallaber, L. M., Fay, P. J., and Bambara, R. A. (1993) Determinants of the RNase H cleavage specificity of human immunodeficiency virus reverse transcriptase, *Nucleic Acids Res. 21*, 4330−4338.
15. DeStefano, J. J., Cristofaro, J. V., Derebail, S., Bohlayer, W. P., and Fitzgerald-Heath, M. J. (2001) Physical mapping of HIV reverse transcriptase to the 5′ end of RNA primers, *J. Biol. Chem. 276*, 32515−32521.
16. DeStefano, J. J. (1995) The orientation of binding of human immunodeficiency virus reverse transcriptase on nucleic acid hybrids, *Nucleic Acids Res. 23*, 3901−3908.
17. Rausch, J. W., and Le Grice, S. F. (2004) "Binding, bending and bonding": polypurine tract-primed initiation of plus-strand DNA synthesis in human immunodeficiency virus, *Int. J. Biochem. Cell Biol. 36*, 1752−1766.
18. Goff, S. P., and Telesnitsky, A. (1997) Reverse transcriptase and the generation of retroviral DNA, in *Retroviruses* (Coffin, J. M., Hughes, S. H., and Varmus, H. E., Eds.) pp 121−160, Cold Spring Harbor Laboratory Press, Cold Spring Harbor, NY.
19. Arts, E. J., and Le Grice, S. F. (1998) Interaction of retroviral reverse transcriptase with template-primer duplexes during replication, *Prog. Nucleic Acid Res. Mol. Biol. 58*, 339−393.
20. Ding, J., Hughes, S. H., and Arnold, E. (1997) Protein-nucleic acid interactions and DNA conformation in a complex of human immunodeficiency virus type 1 reverse transcriptase with a double-stranded DNA template-primer, *Biopolymers 44*, 125−138.
21. Huang, H., Chopra, R., Verdine, G. L., and Harrison, S. C. (1998) Structure of a covalently trapped catalytic complex of HIV-1 reverse transcriptase: implications for drug resistance, *Science 282*, 1669−1675.
22. Sarafianos, S. G., Das, K., Tantillo, C., Clark, A. D., Jr., Ding, J., Whitcomb, J. M., Boyer, P. L., Hughes, S. H., and Arnold, E. (2001) Crystal structure of HIV-1 reverse transcriptase in complex with a polypurine tract RNA:DNA, *EMBO J. 20*, 1449−1461.
23. Boyer, P. L., Ferris, A. L., Clark, P., Whitmer, J., Frank, P., Tantillo, C., Arnold, E., and Hughes, S. H. (1994) Mutational analysis of the fingers and palm subdomains of human immunodeficiency virus type-1 (HIV-1) reverse transcriptase, *J. Mol. Biol. 243*, 472−483.
24. Cristofaro, J. V., Rausch, J. W., Le Grice, S. F., and DeStefano, J. J. (2002) Mutations in the ribonuclease H active site of HIV-RT reveal a role for this site in stabilizing enzyme-primer-template binding, *Biochemistry 41*, 10968−10975.
25. Hughes, S. H., Hostomsky, Z., Le Grice, S. F., Lentz, K., and Arnold, E. (1996) What is the orientation of DNA polymerases on their templates?, *J. Virol. 70*, 2679−2683.
26. Rausch, J. W., Sathyanarayana, B. K., Bona, M. K., and Le Grice, S. F. (2000) Probing contacts between the ribonuclease H domain of HIV-1 reverse transcriptase and nucleic acid by site-specific photocross-linking, *J. Biol. Chem. 275*, 16015−16022.
27. Tisdale, M., Schulze, T., Larder, B. A., and Moelling, K. (1991) Mutations within the RNase H domain of human immunodeficiency virus type 1 reverse transcriptase abolish virus infectivity, *J. Gen. Virol. 72* (Part 1), 59−66.
28. Dudding, L. R., Nkabinde, N. C., and Mizrahi, V. (1991) Analysis of the RNA- and DNA-dependent DNA polymerase activities of point mutants of HIV-1 reverse transcriptase lacking ribonuclease H activity, *Biochemistry 30*, 10498−10506.
29. Julias, J. G., McWilliams, M. J., Sarafianos, S. G., Alvord, W. G., Arnold, E., and Hughes, S. H. (2003) Mutation of amino acids in the connection domain of human immunodeficiency virus type 1 reverse transcriptase that contact the template-primer affects RNase H activity, *J. Virol. 77*, 8548−8554.
30. Julias, J. G., McWilliams, M. J., Sarafianos, S. G., Arnold, E., and Hughes, S. H. (2002) Mutations in the RNase H domain of HIV-1 reverse transcriptase affect the initiation of DNA synthesis and the specificity of RNase H cleavage in vivo, *Proc. Natl. Acad. Sci. U.S.A. 99*, 9515−9520.
31. Rausch, J. W., Lener, D., Miller, J. T., Julias, J. G., Hughes, S. H., and Le Grice, S. F. (2002) Altering the RNase H primer grip of human immunodeficiency virus reverse transcriptase modifies cleavage specificity, *Biochemistry 41*, 4856−4865.
32. Gorshkova, I., Rausch, J. W., Le Grice, S. F., and Crouch, R. J. (2001) HIV-1 reverse transcriptase interaction with model RNA-DNA duplexes, *Anal. Biochem. 291*, 198−206.
33. DeStefano, J. J., Buiser, R. G., Mallaber, L. M., Myers, T. W., Bambara, R. A., and Fay, P. J. (1991) Polymerization and RNase H activities of the reverse transcriptases from avian myeloblastosis, human immunodeficiency, and Moloney murine leukemia viruses are functionally uncoupled, *J. Biol. Chem. 266*, 7423−7431.
34. Kati, W. M., Johnson, K. A., Jerva, L. F., and Anderson, K. S. (1992) Mechanism and fidelity of HIV reverse transcriptase, *J. Biol. Chem. 267*, 25988−25997.
35. Reardon, J. E. (1992) Human immunodeficiency virus reverse transcriptase: Steady-state and pre-steady-state kinetics of nucleotide incorporation, *Biochemistry 31*, 4473−4479.
36. Sambrook, J., and Russell, D. W. (2001) *Molecular Cloning: A Laboratory Manual*, 3rd ed., Cold Spring Harbor Laboratory Press, Cold Spring Harbor, NY.
37. Wöhrl, B. M., Krebs, R., Thrall, S. H., and Le Grice, S. F. J. (1997) Kinetic analysis of four HIV-1 reverse transcriptase enzymes mutated in the primer grip region of p66, *J. Biol. Chem. 272*, 17581−17587.
38. Wöhrl, B. M., Krebs, R., Goody, R. S., and Restle, T. (1999) Refined model for primer/template binding by HIV-1 reverse transcriptase: pre-steady-state kinetic analyses of primer/template binding and nucleotide incorporation events distinguish between different binding modes depending on the nature of the nucleic acid substrate, *J. Mol. Biol. 292*, 333−344.
39. Schatz, O., Cromme, F. V., Gruninger-Leitch, F., and Le Grice, S. F. J. (1989) Point mutations in conserved amino acid residues within the C-terminal domain of HIV-1 reverse transcriptase specifically repress RNase H function, *FEBS Lett. 257*, 311−314.
40. Wu, T., Guo, J., Bess, J., Henderson, L. E., and Levin, J. G. (1999) Molecular requirements for human immunodeficiency virus type 1 plus-strand transfer: analysis in reconstituted and endogenous reverse transcription systems, *J. Virol. 73*, 4794−4805.
41. Wöhrl, B. M., Tantillo, C., Arnold, E., and Le Grice, S. F. (1995) An expanded model of replicating human immunodeficiency virus reverse transcriptase, *Biochemistry 34*, 5343−5356.
42. Cowan, J. A., Ohyama, T., Howard, K., Rausch, J. W., Cowan, S. M., and Le Grice, S. F. (2000) Metal-ion stoichiometry of the HIV-1 RT ribonuclease H domain: evidence for two mutually exclusive sites leads to new mechanistic insights on metal-mediated hydrolysis in nucleic acid biochemistry, *J. Biol. Inorg. Chem. 5*, 67−74.
43. Reardon, J. E., Furfine, E. S., and Cheng, N. (1991) Human immunodeficiency virus reverse transcriptase effect of primer length on template-primer binding, *J. Biol. Chem. 266*, 14128−14134.
44. Brautigam, C. A., and Steitz, T. A. (1998) Structural and functional insights provided by crystal structures of DNA polymerases and their substrate complexes, *Curr. Opin. Struct. Biol. 8*, 54−63.
45. Kunkel, T. A., and Wilson, S. H. (1998) DNA polymerases on the move, *Nat. Struct. Biol. 5*, 95−99.
46. Jacobo-Molina, A., Ding, J., Nanni, R. G., Clark, A. D., Jr., Lu, X., Tantillo, C., Williams, R. L., Kamer, G., Ferris, A. L., Clark, P., et al. (1993) Crystal structure of human immunodeficiency virus type 1 reverse transcriptase complexed with double-stranded DNA at 3.0 Å resolution shows bent DNA, *Proc. Natl. Acad. Sci. U.S.A. 90*, 6320−6324.
47. Fedoroff, O., Salazar, M., and Reid, B. R. (1996) Structural variation among retroviral primer-DNA junctions: solution structure of the HIV-1 (−)-strand Okazaki fragment r(gcca)d(CTGC)·d(GCAGTGGC), *Biochemistry 35*, 11070−11080.
48. Salazar, M., Champoux, J. J., and Reid, B. R. (1993) Sugar conformations at hybrid duplex junctions in HIV-1 and Okazaki fragments, *Biochemistry 32*, 739−744.
49. Salazar, M., Fedoroff, O., Zhu, L., and Reid, B. R. (1994) The solution structure of the r(gcg)d(TATACCC):d(GGGTATACGC) Okazaki fragment contains two distinct duplex morphologies connected by a junction, *J. Mol. Biol. 241*, 440−455.
50. Salazar, M., Fedoroff, O. Y., and Reid, B. R. (1996) Structure of chimeric duplex junctions: solution conformation of the retroviral Okazaki-like fragment r(ccca)d(AATGA).d(TCATTTGGG) from Moloney murine leukemia virus, *Biochemistry 35*, 8126−8135.
51. Zhu, L., Salazar, M., and Reid, B. R. (1995) DNA duplexes flanked by hybrid duplexes: the solution structure of chimeric junctions in [r(cgcg)d(TATACGCG)]2, *Biochemistry 34*, 2372−2380.

52. Egli, M., Usman, N., and Rich, A. (1993) Conformational influence of the ribose 2′-hydroxyl group: crystal structures of DNA-RNA chimeric duplexes, *Biochemistry 32*, 3221−3237.
53. Egli, M., Usman, N., Zhang, S. G., and Rich, A. (1992) Crystal structure of an Okazaki fragment at 2-Å resolution, *Proc. Natl. Acad. Sci. U.S.A. 89*, 534−538.
54. Dudding, L. R., and Mizrahi, V. (1993) Rapid kinetic analysis of a point mutant of HIV-1 reverse transcriptase lacking ribonuclease H activity, *Biochemistry 32*, 6116−6120.
55. Wisniewski, M., Balakrishnan, M., Palaniappan, C., Fay, P. J., and Bambara, R. A. (2000) Unique progressive cleavage mechanism of HIV reverse transcriptase RNase H, *Proc. Natl. Acad. Sci. U.S.A. 97*, 11978−11983.
56. Wisniewski, M., Balakrishnan, M., Palaniappan, C., Fay, P. J., and Bambara, R. A. (2000) The sequential mechanism of HIV reverse transcriptase RNase H, *J. Biol. Chem. 275*, 37664−37671.
57. Joshi, P., and Prasad, V. R. (2002) Potent inhibition of human immunodeficiency virus type 1 replication by template analog reverse transcriptase inhibitors derived by SELEX (systematic evolution of ligands by exponential enrichment), *J. Virol. 76*, 6545−6557.
58. Joshi, P. J., North, T. W., and Prasad, V. R. (2005) Aptamers directed to HIV-1 reverse transcriptase display greater efficacy over small hairpin RNAs targeted to viral RNA in blocking HIV-1 replication, *Mol. Ther. 11*, 677−686.

BI051770W